

RESEARCH

Open Access



Experimental Investigation on Fatigue Improvement of Orthotropic Steel Bridge Deck Using Steel Fiber Reinforced Concrete

Huawen Ye^{1,2*} , Ao Huang¹, Chengchuan Jiang¹ and Wenchao Wang¹

Abstract

The high-performance topping concrete overlay would significantly reduce the fatigue stresses at susceptible details of orthotropic steel deck (OSD) and effectively improve the fatigue performance. Full-scale fatigue tests and numerical simulations were carried out to quantify the effects of steel fiber reinforced concrete (SFRC) topping pavement in reducing the OSD fatigue stresses based on a practical bridge design. Fatigue stress of the OSD critical details was measured from tests and cracking was observed in the SFRC overlay. Both an innovative pre-pump-pulse Brillouin optical time domain analysis (PPP-BOTDA) distributed optical fiber sensor and strain gauges were also used to measure the stress at OSD fatigue-prone details, including the crossbeam cut-out, rib-to-deck weld, rib-to-crossbeam weld and splice of U-rib. The corresponding three-dimensional (3-D) finite element model was then established and verified by the test results, and used to conduct a parametric study to obtain a quantitative expression of fatigue stress reduction factor, in terms of relative elastic modulus and thickness of overlay and steel deck plate. The proposed quantitative model of the fatigue stress reduction effect can guide the cost-effective design of composite bridge deck.

Keywords Composite bridge deck, SFRC, Full-scale test, Fatigue stress reduction factor, PPP-BOTDA

1 Introduction

The orthotropic steel deck (OSD) system is fabricated by a steel deck plate stiffened by longitudinal U-ribs and supported by transverse crossbeams. It has been widely acknowledged as an excellent solution for suspension bridge and cable-stay bridge structures where self-weight is a critical issue. However, numerous studies (Fisher & Barsom, 2016; Ju et al., 2018; Kainuma et al., 2015; Ke et al., 2021; Maljaars & Paulissen, 2016; Yamada et al.,

2005) had reported that OSD structures beneath heavy vehicle lanes are susceptible to fatigue cracking, delamination, and deterioration of the thin wearing surface. This fatigue failure is attributed to the localized effects of wheel loads (Deck et al., 2012). Consequently, researchers have focused on cost-effective ways to enhance the local stiffness of OSD, which has been a topic of study for decades.

For many years, it has been widely recognized that the overlay plays a significant role in the stress behavior of fatigue-prone details by diffusing local wheel loads and participating in the local bending of the OSD (Inokuchi et al., 2010). Thus, the steel-concrete composite concept has become a promising solution to the fatigue cracking of OSD bridges by combining the advantages of both steel and concrete materials. In recent years, there have been renovations in high-performance steel fiber reinforced concrete (SFRC), which exhibits higher ductility

Journal information: ISSN 1976-0485 / eISSN 2234-1315

*Correspondence:

Huawen Ye

hbha2000@163.com

¹ School of Civil Engineering, Southwest Jiaotong University, Chengdu 610031, China

² National Key Laboratory of Bridge Intelligent and Green Construction, Southwest Jiaotong University, Chengdu 611756, Sichuan, China

than conventional concrete (Krstulovic et al., 1995). The addition of a SFRC overlay has demonstrated a substantial reduction in fatigue stresses of the OSD structures through numerical simulation (Walter et al., 2007), experiments (Ishii et al., 2013; Jiang et al., 2017; Liu et al., 2020; Murakoshi et al., 2012, 2013; Noguchi et al., 2016; Ono et al., 2005, 2009) and engineering applications (Kodama et al., 2010; Miki et al., 2006). Based on the concrete properties and layer thicknesses, the applications of overlays can be categorized into two major alternatives: (i) ordinary strength SFRC with thicker layer (75–150 mm), including commonly used SFRC (Ishii et al., 2013; Krstulovic et al., 1995; Murakoshi et al., 2012, 2013; Noguchi et al., 2016; Ono et al., 2005, 2009; Walter et al., 2007) or engineered cementitious composite (ECC) (Liu et al., 2020); (ii) high-strength SFRC with thin layer (30–50 mm), such as ultra-high performance concrete (UHPC) (Abdelbaset et al., 2020; Dieng et al., 2013; Pei et al., 2018). Although the thin overlay is popular for large-scale structures due to weight considerations, it increases construction costs and durability issues. Field measurements (Pei et al., 2018) of the effects of a thin UHPC layer (50 mm thickness) on the fatigue stress of OSD details showed that the thin UHPC layer has a significant impact on the stresses at the rib-to-deck weld and the rib splice weld, but a slight influence on the cut-out of the crossbeam web. Test results (Abdelbaset et al., 2020) also showed the application of a 60-mm UHPC layer reduced the hot spot stresses by 26–83% at the OSD details. Ye et al., (2017, 2021, 2022) found that overlay cracking governs the fatigue failure modes of steel–concrete composite deck, and both the flexural strength and thickness of concrete overlay are controlling factors. These engineering explorations revealed that there is an optimal matching of the concrete grade and overlay thickness, which leads to the most economical and reasonable composite with high fatigue resistance. However, few systematic research studies have been conducted using comparative tests to accurately quantify the stress reduction effect of the overlay on the OSD and guide the cost-effective design of the concrete overlay for the composite deck.

In this study, a full-scale composite deck specimen was fabricated and investigated to characterize the quantitative effect of SFRC overlay on reducing fatigue stress of OSD. The fatigue stress measurements were carried out using both strain gauges and a high-resolution PPP-BOTDA distributed optical fiber sensor, which is a popular and adaptable technology for measuring the strain field of structures. In addition, a parametric stress analysis using finite element (FE) modeling was performed to obtain the fatigue stress reduction factor by considering a variety of elastic modulus and thicknesses of concrete

overlay in the composite deck design. The study aimed to achieve the objectives as: (1) compare fatigue stress measurements at the critical OSD details with and without SFRC overlay; (2) identify critical factors that contribute to the SFRC overlay's reducing effect through FE modeling; and (3) propose a quantitative expression of the fatigue stress reduction factor using the relative elastic modulus and thickness of the overlay and steel deck plate.

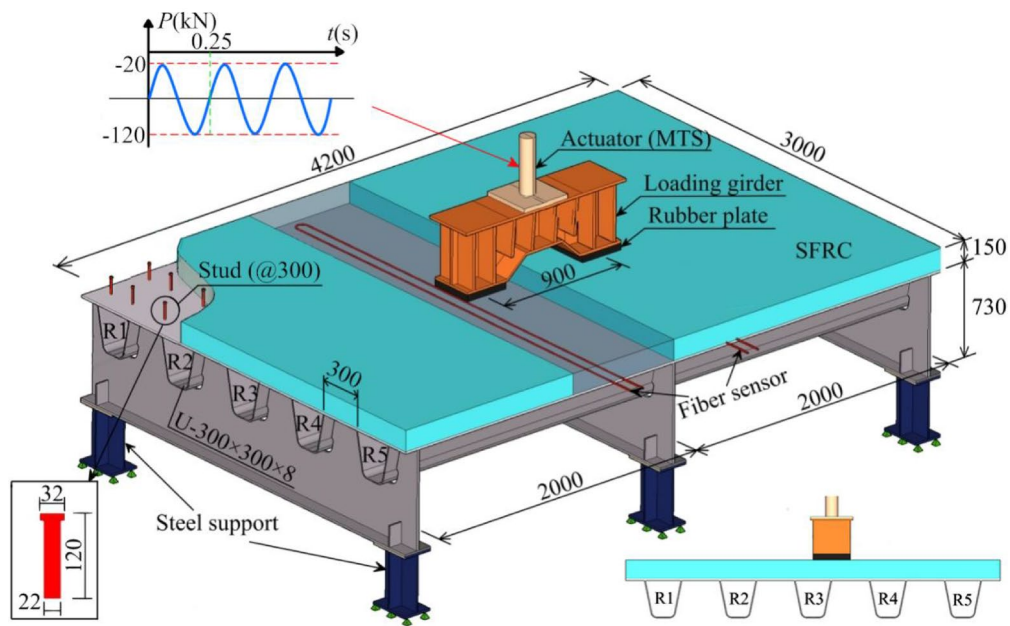
2 Full-Scale Experimental Investigation and Numerical Simulation

2.1 Full-Scale Composite Deck Specimen

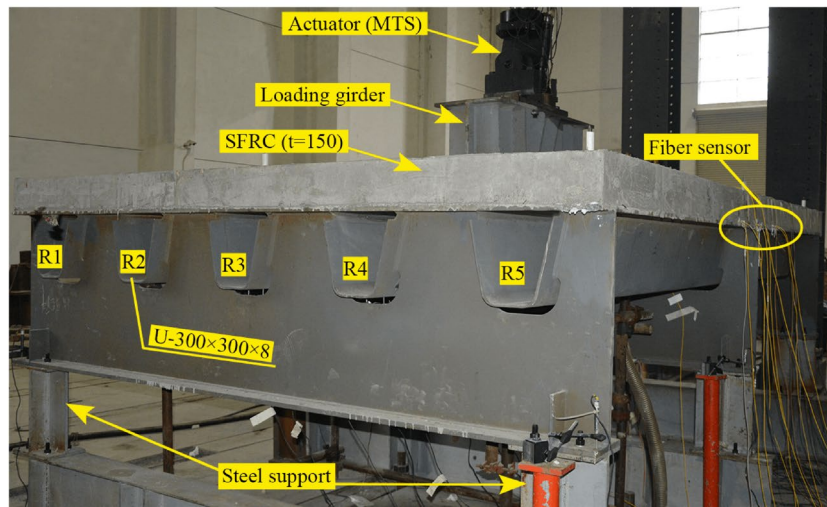
Based on European and Chinese Standards (ECS, 2005; MTPRC, 2015), a prototype specimen with SFRC overlay was designed for a cable-stayed bridge across the Yangtze River in Yibin, China. The full-scale specimen comprised three crossbeams spaced 2 m apart and five U-ribs spaced 300 mm apart, as shown in Fig. 1. The deck plate was 16 mm thick, and the U-rib was 300 mm wide, 300 mm high, and 8 mm thick. The crossbeams had an 18-mm-thickness web. The specimen was placed on six short columns and connections were made using bolts. The steel fabrication and concrete casting were performed to meet the same level of quality achieved in realistic industrial conditions in China, and tolerances and welding satisfied the requirements of the standards (ECS, 2005; MTPRC, 2015).

The testing aimed to investigate the local response of the composite deck under wheel loads and the interactions between the OSD and the SFRC overlay. The global response due to dead load was assumed to have a minor impact on fatigue performance and was therefore ignored. Fatigue stress analysis of the realistic composite bridge deck was conducted under 100-year traffic loading using Fatigue Load Model 3 (ECS, 2005; MTPRC, 2015). A constant fatigue loading of two million cycles of 100 kN (with maximum and minimum loads of 120 and 20 kN, respectively) was determined to replicate the actual in-service stress range. The loading was applied to two 300 mm × 300 mm surfaces using a loading girder, and the fatigue loading frequency was 4 Hz. Two rubber plates measuring 300 mm × 300 mm were also used as loading patches to ensure uniform contact under the actuator.

To measure the fatigue stress reduction effect of the SFRC overlay, a static test was conducted on the OSD specimen without the overlay to obtain the principal tensile stresses at critical locations, which were considered as the reference fatigue stress, σ_0 , as shown in Fig. 2a. Next, the specimen with SFRC overlay was tested to obtain the corresponding principal tensile stresses at the same critical locations of the OSD, which were considered as the



(a) Schematic test setup of composite deck (unit: mm)



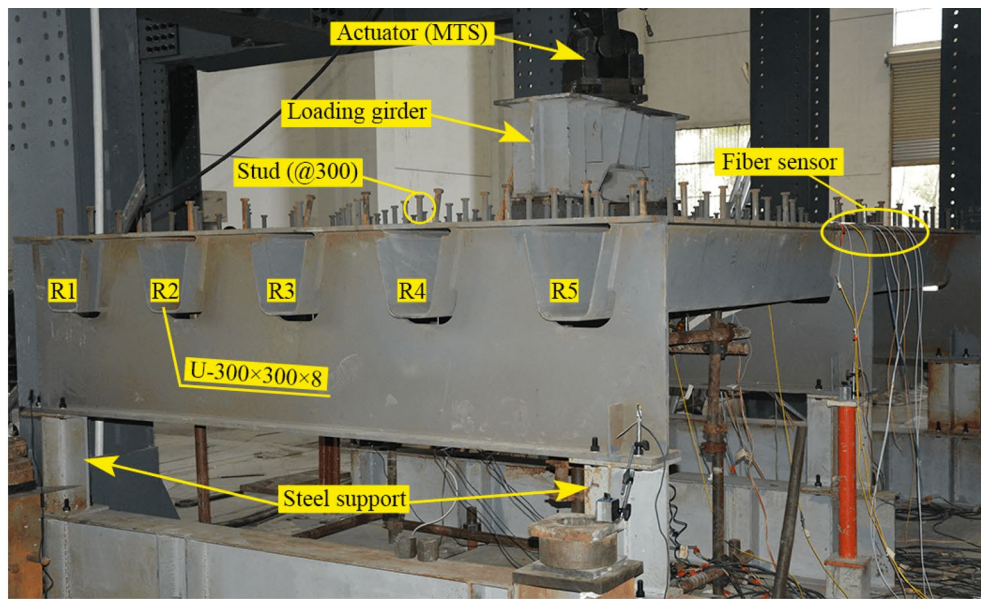
(b) Fatigue loading on composite deck specimen

Fig. 1 Fatigue test of full-scale composite deck specimen

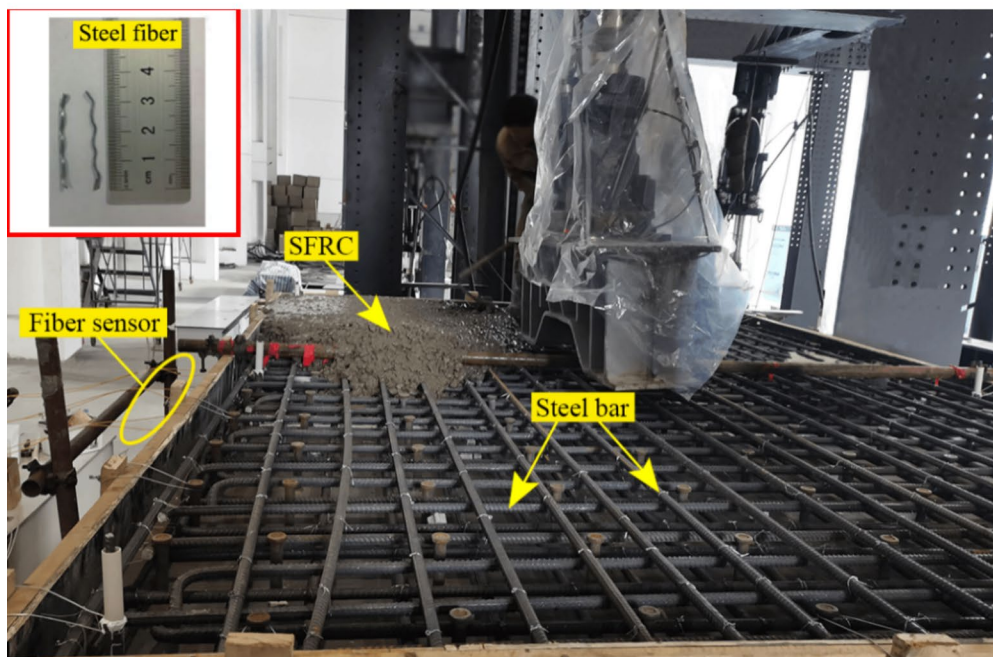
reduced fatigue stress, σ_1 , after applying the SFRC overlay, shown in Fig. 2b.

The deck plate and the concrete overlay were connected by headed studs which had a diameter of 22 mm, a height of 120 mm and a head diameter of 32 mm. The stud supplier provided that the yield strength and tensile strength for the 22-mm-diameter stud exceed 320 MPa and 400 MPa, respectively. The shear stiffness of the stud was determined to be 160 kN/mm from the push-out test. The SFRC had a cubic compressive

strength, f_{cu} , of 53.0 MPa (equivalent to C50 grade in China standard), and was made using corrugated steel fibers with a volume fraction of 50 kg/m^3 (corresponding to a fiber volume fraction, V_f , of 0.63). The steel fibers had a total length of 35 mm and a diameter of 0.7 mm (giving a fiber aspect ratio of 50), and an average tensile strength of 1100 MPa. The concrete overlay also included double-layer mesh reinforcements made of 20-mm-diameter steel rebar with a nominal tensile strength of 400 MPa (HRB400 in China standard), as



(a) Static contrast test of pure OSD (without overlay)



(b) SFRC cast on the deck plate

Fig. 2 Static test of pure OSD before SFRC cast

Table 1 Properties of components in composite deck

Properties	Q345qD steel	SFRC (0.63 vol. %)
Modulus of elasticity (GPa)	206	34.5
Poisson's ratio	0.3	0.167
Thickness (mm)	–	150

shown in Fig. 2b. Table 1 summarizes the mechanical properties of the specimen.

2.2 Stress Distribution Measurement Using Distributed Optical Fiber Sensor

An innovative and commercially available PPP-BOTDA distributed optical fiber sensor (NBX-7000 hybrid sensing

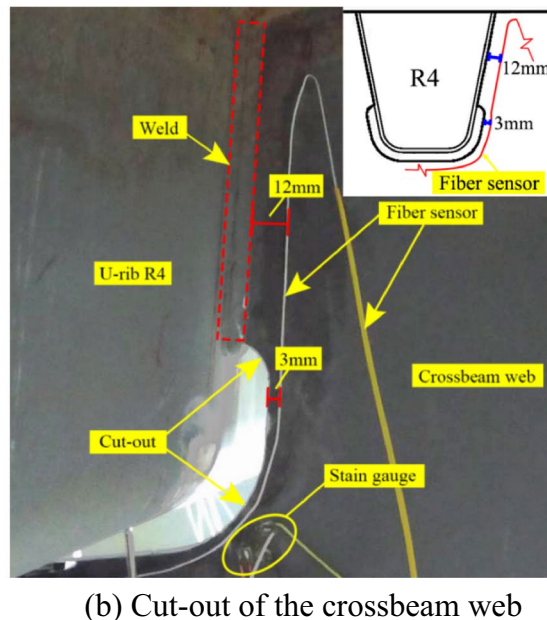
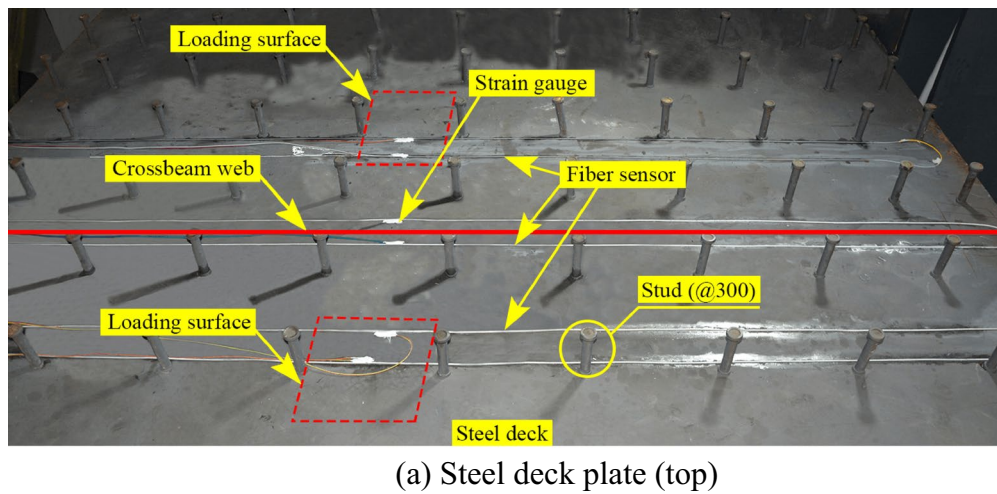


Fig. 3 PPP-BOTDA optical fiber sensor attached on the steel deck

system) was used to measure the distributed strain values of the upper surface of the steel deck plate and the cut-out of the crossbeam, as illustrated in Fig. 3. A telecommunication-type optical fiber was pretensioned and then adhered to the steel surface using epoxy to serve as the distributed sensor. The PPP-BOTDA sensor provides high spatial resolution of 1 cm and is capable of automatically removing the thermo-optical effects on strain. It has a strain range of 30,000 microstrains and an error in measurement of approximately ± 10 microstrains. The sensor measures the total deformation along the length of the optical fiber and averages the strains over a spatial resolution of 1 cm.

The Brillouin sub-system of the NBX-7000 hybrid sensing system utilizes the PPP-BOTDA technology, while the Rayleigh sub-system employs Tunable Wavelength Coherent Optical Time Domain Reflectometry (TW-COTDR). For standard, single-mode fiber, the hybrid system provides frequency shifts for both Brillouin and Rayleigh scatterings. Since both shifts are a function of strain and temperature, their separation is necessary to remove the influence of temperature on strain and vice versa, which allows for obtaining pure strain and temperature values. The principles of PPP-BOTDA and TW-COTDR are demonstrated in Fig. 4.

To monitor the strain at the fatigue-prone positions, such as the crossbeam cut-out, rib-to-deck weld,

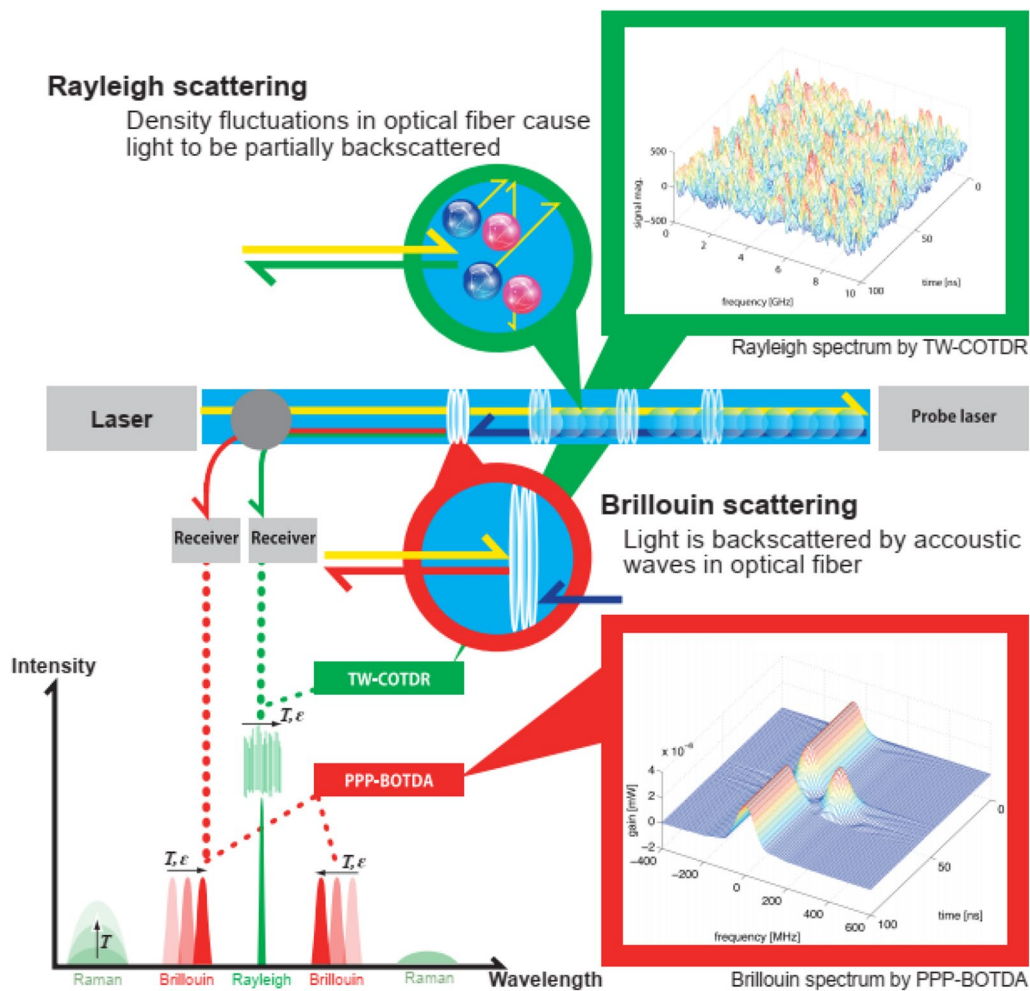


Fig. 4 Principles of PPP-BOTDA and TW-COTDR

rib-to-crossbeam weld, and splice of U-rib, an independent monitor was also used. The strains were monitored by not only the optical fiber sensor, but also simultaneously measured by high-precision strain gauges of TDS-540 from Tokyo measuring instruments Lab. The principal tensile stresses were measured by the strain gauges located at the fatigue-prone details of the steel deck, such as the rib-to-deck welded connection, cut-out detail in the web of the crossbeam, and splice of U-rib, as shown in Fig. 5. The strain gauges were placed at 5 mm away from the weld toe or the edge of the cut-out. Displacement sensors were also placed on the bottom of the deck underneath the loading position.

2.3 FE Modeling

A 3-D finite element (FE) model of the full-scale specimen was created and analyzed under monotonic load using the professional program ANSYS 17.0, as depicted in Fig. 6. The steel deck was modeled as a linear and

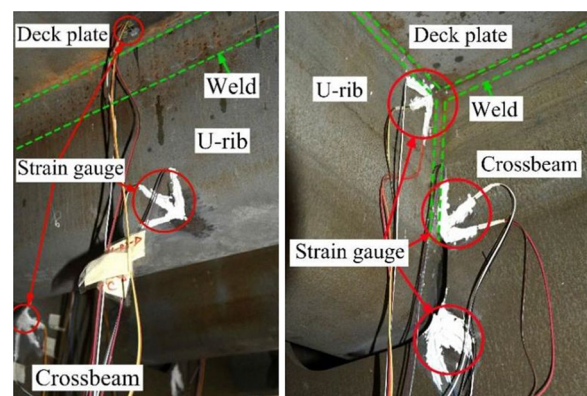


Fig. 5 Strain gauges at details

isotropic material using SHELL 63, while the concrete overlay was modeled as a nonlinear and isotropic material using SOLID 65. The steel–concrete interface

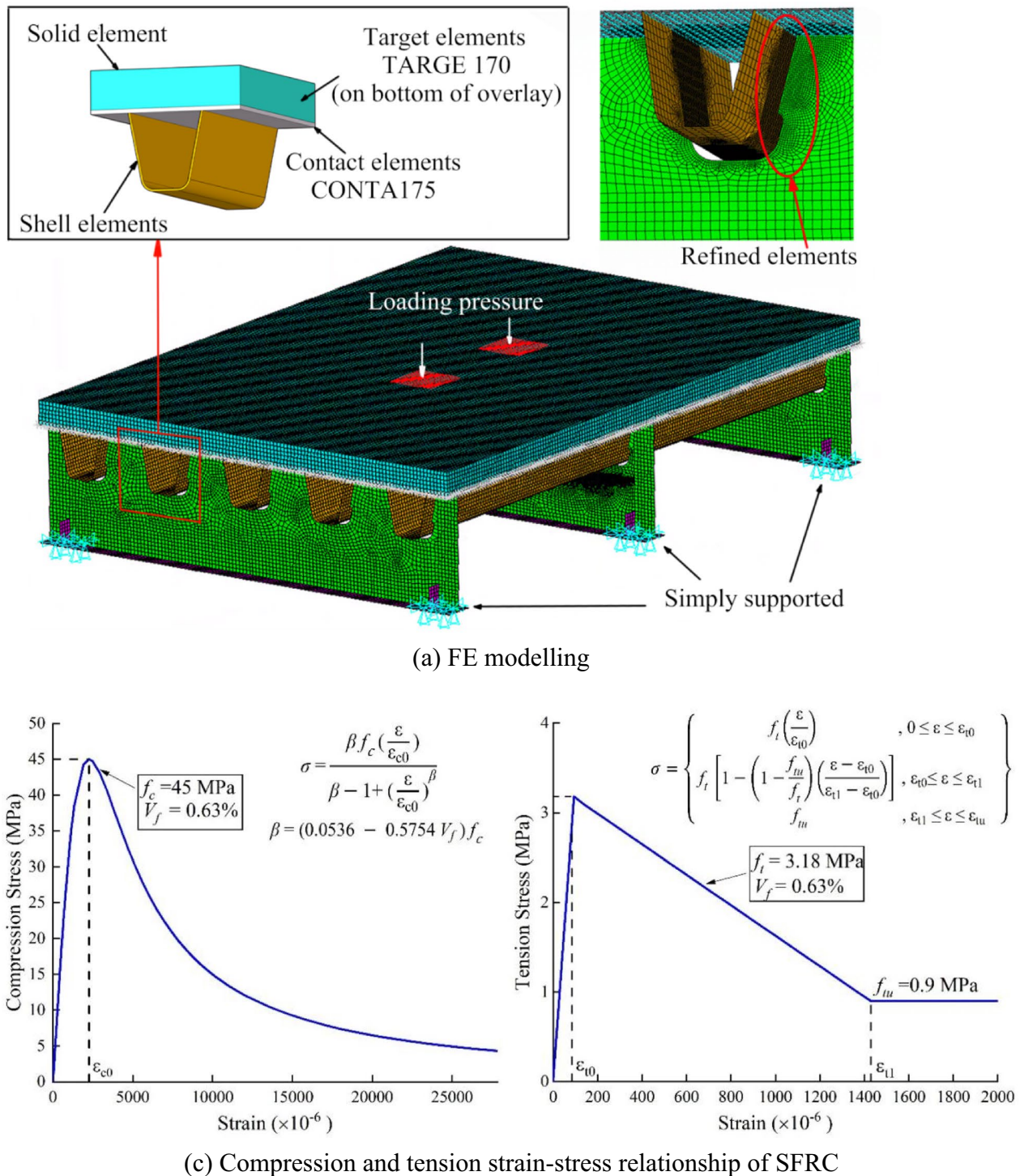


Fig. 6 3D FE modeling for composite deck

behavior was simulated as a contact condition using a contact pair consisting of CONTA175 and TARGE 170 elements. The constraint set only included transitional degrees of freedom, and the effect of shell thickness and

separation between overlay and steel deck were excluded. The studs were modeled using the spring element COMBIN14 with equal normal and shear stiffness in the test. The element size was refined to 1.0 mm in the focused

zones of the considered fatigue details, while the size of 5 mm was used outside of these zones based on the precision requirement determined through trial and error. A load pressure of 100 kN/(2×300 mm×300 mm), corresponding to a wheel with two axle loads, was applied on top of the overlay. Fig. 6a illustrates that only translational degrees of freedom (DOFs) were restrained at the bolting position on both ends of the three crossbeams. The restrained area at each end was 200 mm×200 mm.

The mechanical properties of the components were based on Fig. 6b and Table 1 in the numerical simulation. A nonlinear constitutive relation model was used to represent the material characteristics of SFRC. The compressive stress–strain relationship of SFRC was expressed as shown in Fig. 6b based on the study (Luiz et al., 2010), where σ_c and f_c (approximately $0.85f_{cu}$) are the compressive stress and the cylinder strength, respectively, ϵ_c is strain, ϵ_{c0} is the peak strain, and β is the factor in terms of the fiber volumetric fraction V_f . The tensile stress–strain relationship model of SFRC, as described by Lok and Xiao (1999), is shown in Fig. 6b, where f_t is the ultimate tensile strength, ϵ_{t0} is the ultimate strain, and f_{tu} is defined as the residual strength with respect to V_f .

3 Results and Discussion

3.1 Deformation and Cracking Under Wheel Loading

The deflection, f , was analyzed using the established FE model of the composite deck beneath the loading surface. Figs. 7 and 8 show a comparison between the experimental and numerical deflections at the bottom of the deck, with the deflection, f_1 , for the case with overlay being approximately half that of the case without overlay, f_0 . The effect of the overlay in reducing local deformation under wheel loading was significant. The comparison shows good agreement between the test and predicted deflections, confirming the validity of the finite element model for analyzing the behavior of the composite structure. A slight relative displacement (less than 0.01 mm) between the SFRC overlay and the steel deck was observed in the experiment due to the strong arrangement of headed-stud connections at the steel–concrete interface.

After approximately 10,000 cycles of fatigue loading, cracking was observed in the concrete overlay (represented by the red curves), while no cracking was found in the steel deck. Throughout the fatigue test, crack width and depth were continuously measured, revealing that the cracking occurred only in the reinforcement cover, with a final maximum depth of approximately 25 mm and a maximum width of less than 0.15 mm, as depicted in Fig. 9. This phenomenon can be attributed to the retardation of the steel fiber and the steel rebars within the

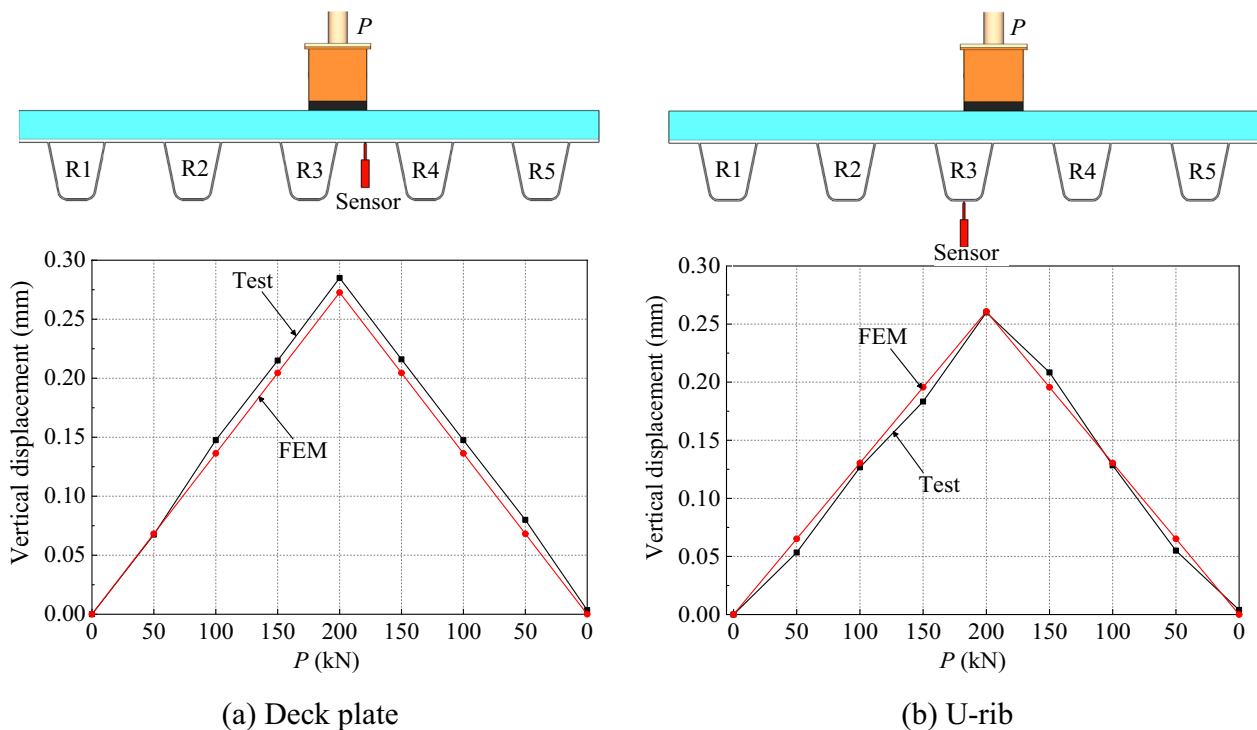


Fig. 7 Load–displacement curves

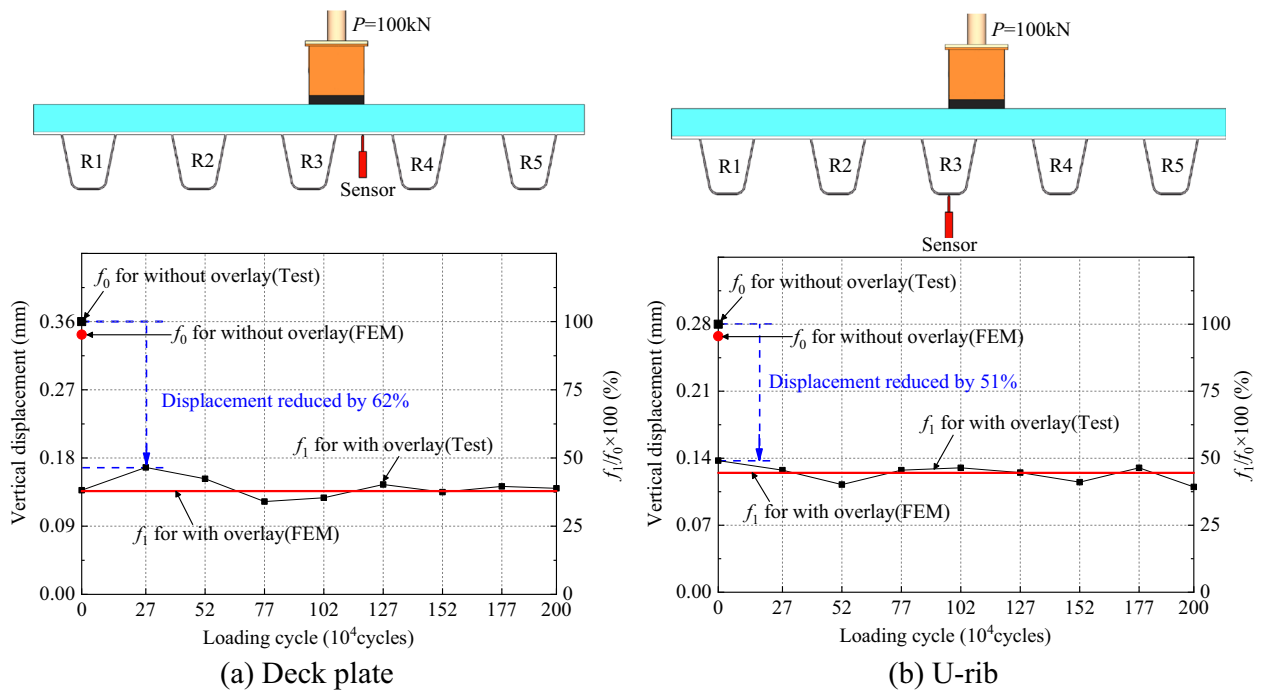


Fig. 8 Time history of deflection under fatigue loading

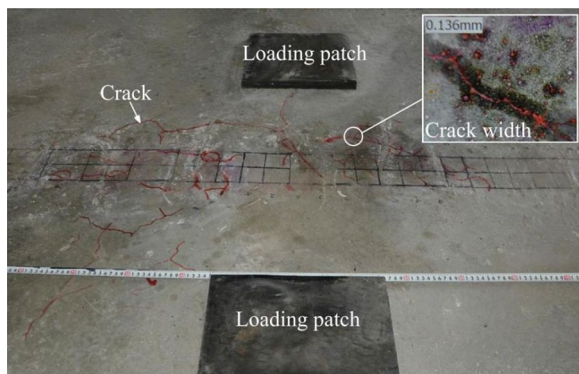


Fig. 9 Overlay cracking after fatigue loading

concrete. The limited cracking of the overlay had only a minor impact on local deformations and fatigue stresses, as illustrated in Figs. 8 and 9.

3.2 Fatigue Stress of Steel Deck

Strain gauges were utilized to investigate the effect of the overlay on the principal tensile stresses at fatigue-prone details of welded connections, including the crossbeam cut-out, rib-to-crossbeam weld, rib-to-deck weld, and splice of U-rib. The unfavorable principal tensile stresses at identical and critical locations of specimens with and without overlay, σ_1 and σ_0 , are compared and summarized in Fig. 10.

The ratio of unfavorable principal tensile stresses with and without overlay, σ_1/σ_0 , was defined as the fatigue stress reduction factor and served as an indicator of the SFRC overlay’s reducing effect. The results demonstrate that the application of a 150-mm-thick SFRC layer significantly reduced the fatigue stresses at the considered locations. The reduction factors were over 75% for stress at the rib-to-deck and rib-to-crossbeam weld, whereas the reduction factors were approximately 40% at locations of cut-out and splice of U-rib. Therefore, the fatigue stresses at the rib-to-deck and rib-to-crossbeam weld are more sensitive to the overlay than those at the cut-out and splice of U-rib. Additionally, it was observed that the numerical and experimental stresses of the composite specimen were in good agreement, and the established FE model can be used to conduct quantitative analysis of the stress-reducing effect of SFRC for composite deck design.

3.3 Stress Distribution Measured by PPP-BOTDA

Fig. 11 illustrates stress distributions along the cross-beam cut-out and the top of the steel deck plate detected by the PPP-BOTDA sensors for cases with and without overlay. The FE simulation results are also presented. Due to the need for pretensioning, the optical fiber could not be applied in the rib-to-crossbeam weld and rib-to-deck weld in this test. It is evident that the addition of a

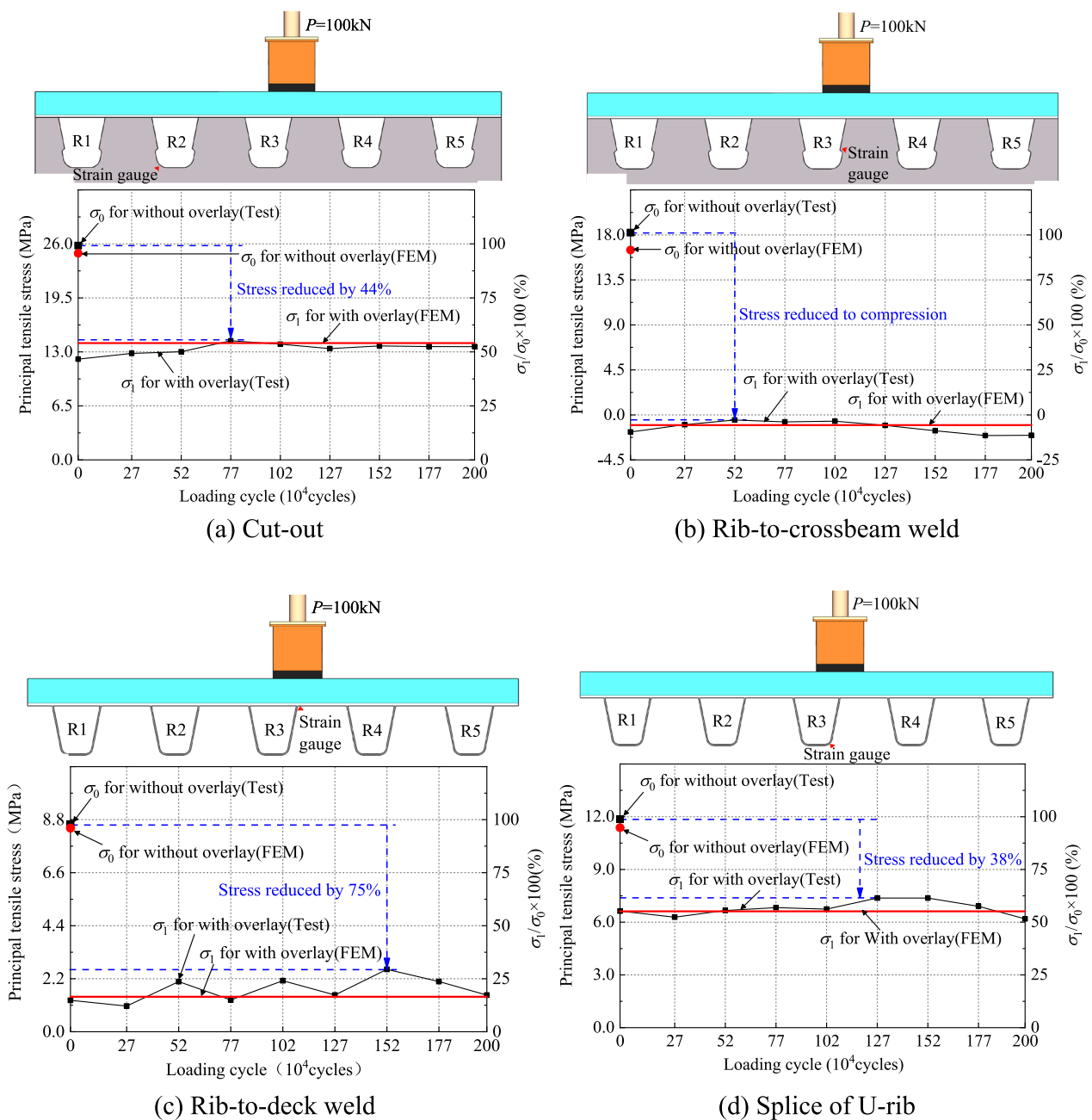


Fig. 10 Time history of principal tensile stresses at fatigue-prone details of OSD

150 mm SFRC overlay can significantly reduce the stress amplitudes and fluctuations of the considered locations.

In addition to the spot stress reduction of fatigue-prone details in Figs. 10, 11b demonstrates that the significant reduction also occurred in the stress field of the OSD. The transfer of a local wheel load starts from the deck plate to the supporting U-rib walls, and the localized response is governed by the spacing of the rib walls and the relative stiffness (thickness) of the deck

plate and U-ribs. It should be noted that the fatigue stresses (wheel-induced stresses) created by this localized mechanism are sensitive to the size of the wheel patch load and any load diffusion through the wearing surface. The topping concrete overlay substantially decreases the relative stiffness (thickness) of the deck plate and U-ribs while substantially increasing the size of the wheel patch load. Therefore, the fatigue stresses

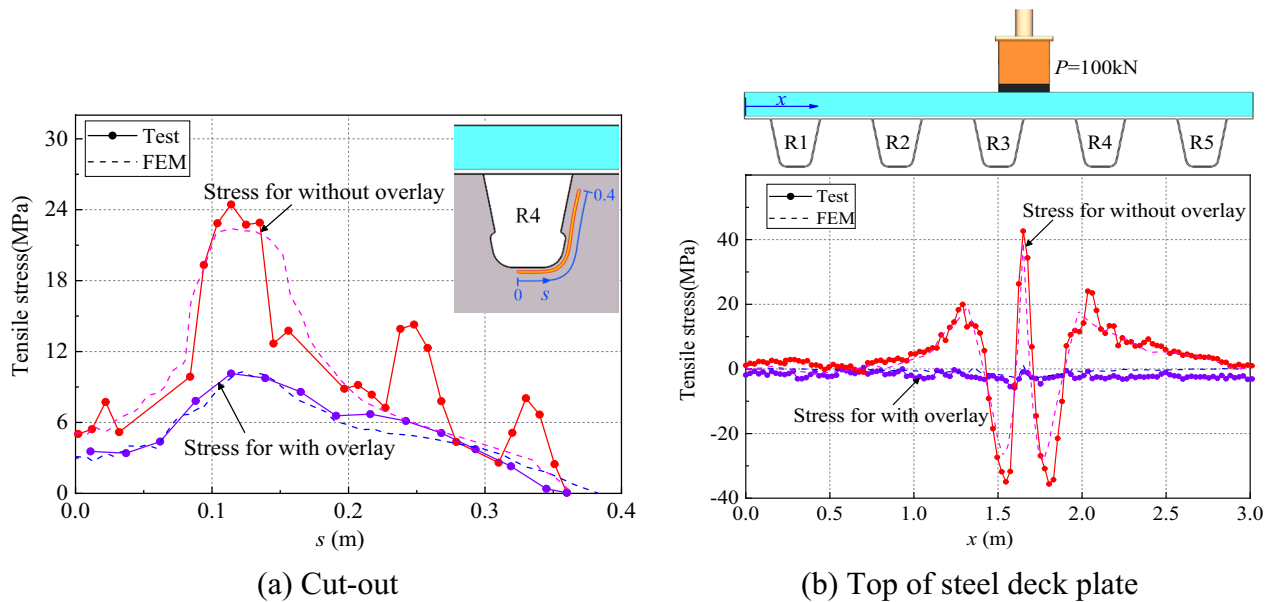


Fig. 11 Measured stress distribution by the PPP-BOTDA

of the composite deck can be much lower than those of the conventional OSD.

3.4 Fatigue Stress Reduction Factor

Note that the thickness of steel deck plates used in conventional U-rib stiffener OSDs varies from 12 to 18 mm, and the structural arrangements regarding section properties also vary slightly among European and Chinese steel bridges (ECS, 2005; MTPRC, 2015). As these types and dimensions have proven to be effective and cost-efficient, a benchmark configuration of 300-mm-spaced U-ribs with a stiffener of (300×300×8 mm) and an 18-mm-thick deck plate can be used to obtain the fatigue stress reduction factor in terms of elastic modulus and thickness of the overlay and steel deck plate through the established FE model. E_s , E_c and t_s , t_c are elastic modulus and thickness of steel deck plate and SFRC overlay, respectively. The elastic modulus and thickness of the steel deck plate, E_s and t_s , respectively, were kept constant as defined in the test. The common ranges of two key design parameters were considered for concrete in the parametric analysis in the composite deck as: (a) t_c ranging from 30 to 150 mm; and (b) E_c varying from 0.5 to 40 GPa.

The numerical results of the fatigue stress reduction factor were fitted to an exponential equation using the Levenberg Marquardt optimization algorithm, which is expected to be universal and convenient for determining the material and corresponding thickness of the overlay to satisfy the design requirements of the composite deck. Fig. 12 illustrates the fitting curves for the crucial details

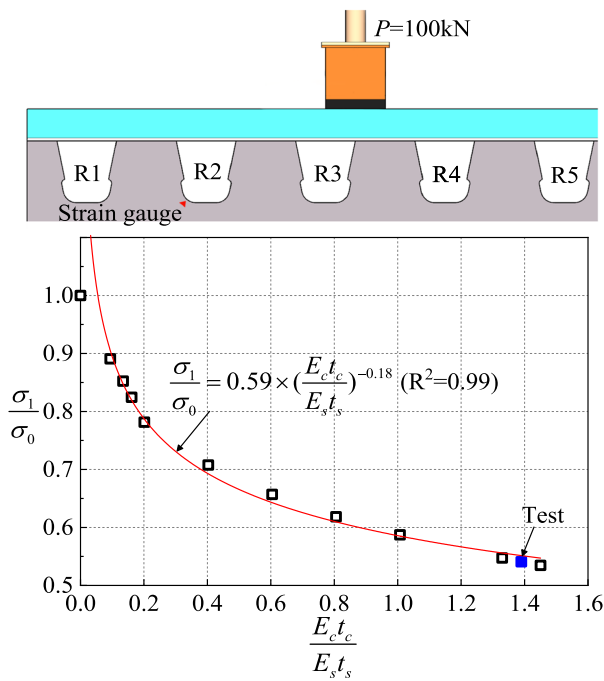
of crossbeam cut-out, rib-to-crossbeam weld, rib-to-deck weld, and splice of U-rib. Table 2 also summarizes the constants of the fitting equations for the critical details.

It should be noted that the rate of change in the fatigue stress reduction factor decreases as the overlay stiffness increases and gradually approaches an approximate standstill when the overlay stiffness approaches that of the steel deck plate [$E_c t_c / (E_s t_s) = 1$]. Large overlay thickness and high concrete elastic modulus (corresponding to the concrete grade) increase the construction cost; therefore, in terms of fatigue verification of the composite deck, the proposed fatigue stress reduction factor can guide the optimum design of the composite deck.

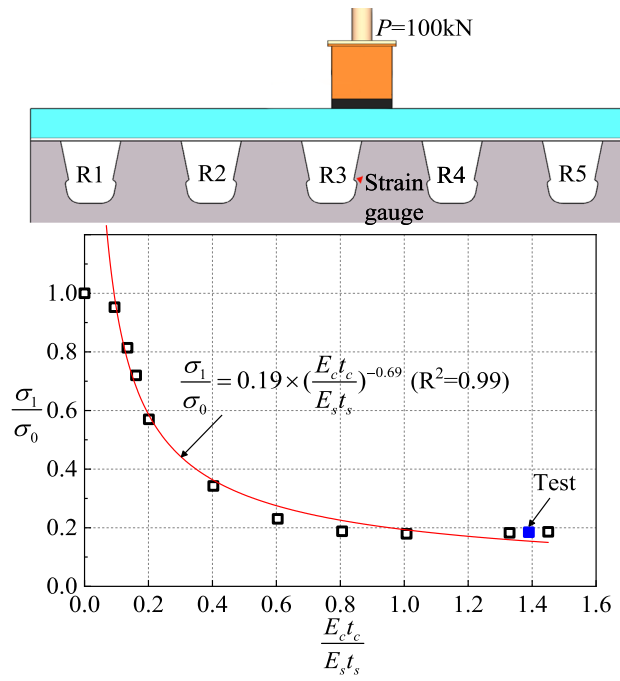
4 Conclusion

The fatigue reducing effects of a concrete overlay on the composite deck were investigated both experimentally and numerically, focusing on fatigue-prone details. Full-scale fatigue tests were conducted on a specimen with a 150 mm SFRC overlay to quantify the reduction in principal tensile stresses under wheel loading. A 3D FE model was also developed to simulate the fatigue response of the specimen and obtain the fatigue stress reduction factor for each critical detail under varying stiffness of overlay and steel deck. The following conclusions were drawn:

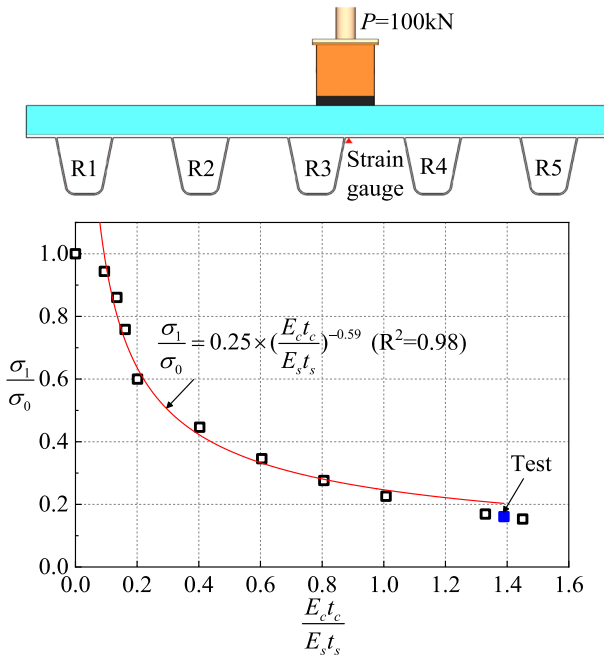
- The high-performance concrete overlay showed early cracking under fatigue loading, but the steel fibers and reinforcement helped to confine crack width



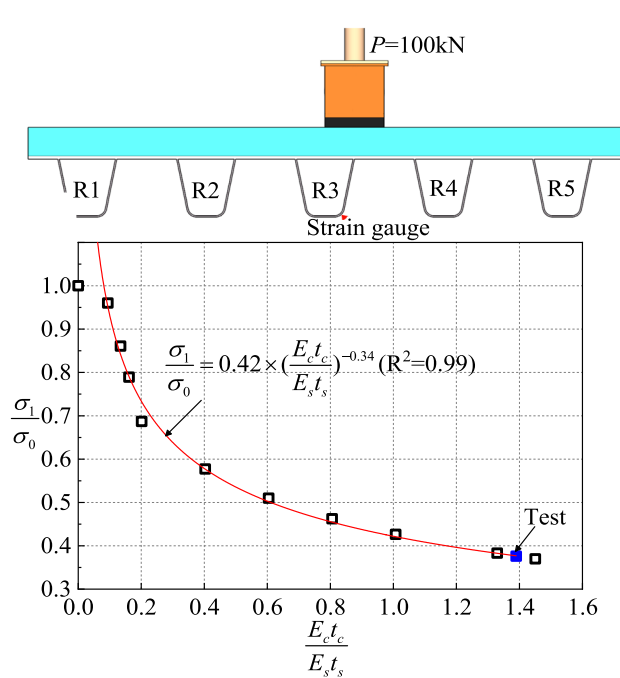
(a) Cut-out



(b) Rib-to-crossbeam weld



(c) Rib-to-deck weld



(d) Splice of U-rib

Fig. 12 Fatigue stress reduction factors at fatigue-prone details of the composite deck

and depth. Even with cracks not exceeding the depth of the concrete cover, the 150 mm SFRC overlay reduced local deflection and principal tensile stresses

at all considered fatigue-prone details of OSD by over 40%.

- Among the fatigue-prone details of crossbeam cut-out, rib-to-deck weld, rib-to-crossbeam weld, and

Table 2 Summary of fatigue stress reduction factors in composite deck

Equation	Detail	α	β
$\frac{\sigma_1}{\sigma_0} = \alpha \times \left(\frac{E_{cfc}}{E_{stf_s}} \right)^\beta$	Cut-out	0.59	- 0.18
	Rib-to-crossbeam weld	0.19	- 0.69
	Rib-to-deck weld	0.25	- 0.59
	Splice of U-rib	0.42	- 0.34

splice of U-rib, the rib-to-deck weld detail showed the highest sensitivity to the concrete overlay in terms of fatigue stress reduction.

- The proposed equation for the fatigue stress reduction factor, in terms of relative elastic modulus and thickness of the SFRC overlay and steel deck plate, could guide cost-effective design of steel–concrete composite bridge decks.

The current FE study did not consider the effects of steel rebars, which should be addressed in further investigations.

Acknowledgements

The authors would like to acknowledge the financial support by the National Natural Science Foundation of China (No. 51208430, 52278219).

Author contributions

HY: conceptualization, methodology, writing; AH: data analysis, validation; CJ: reviewing and editing; WW: experiments. All authors read and approved the final manuscript.

Author's information

Huawen Ye: Associate Professor, School of Civil Engineering and National Key Laboratory of Bridge Intelligent and Green Construction, Southwest Jiaotong University, Chengdu 610031, China.

Ao Huang: Master student, School of Civil Engineering, Southwest Jiaotong University, Chengdu 610031, China.

Chengchuan Jiang: Master student, School of Civil Engineering, Southwest Jiaotong University, Chengdu 610031, China.

Wenchao Wang: Master student, School of Civil Engineering, Southwest Jiaotong University, Chengdu 610031, China.

Funding

The authors would like to confirm the financial support by the National Natural Science Foundation of China (No. 51208430, 52278219).

Availability of data and materials

The raw/processed data required to reproduce these findings cannot be shared at this time due to legal or ethical reasons.

Declarations

Ethics approval and consent to participate

Not applicable.

Consent for publication

All authors have seen the manuscript and approved to submit to your journal.

Competing interests

We declare that we have no financial and personal relationships with other people or organizations that can inappropriately influence our work, there

is no professional or other personal interest of any nature or kind in any product, service and/or company that could be construed as influencing the position presented in, or the review of, this manuscript.

Received: 26 December 2022 Accepted: 17 April 2023

Published online: 25 July 2023

References

- Abdelbaset, H., Cheng, B., Tian, L., Li, H., & Zhang, Q. (2020). Reduce hot spot stresses in welded connections of orthotropic steel bridge decks by using UHPC layer: Experimental and numerical investigation. *Engineering Structures*, 220(C), 1–16. <https://doi.org/10.1016/j.engstruct.2020.110988>
- Deck, B., Robert, C., & John, F. (2012). *Manual for design, construction, and maintenance of orthotropic steel deck bridge*. FHWA IF.
- Dieng, L., Marchand, P., Gomes, F., Tessier, C., & Toutlemonde, F. (2013). Use of UHPFRC overlay to reduce stresses in orthotropic steel decks. *Journal of Constructional Steel Research*, 89(Oct), 30–41. <https://doi.org/10.1016/j.jcsr.2013.06.006>
- ECS. (2005). *Eurocode 3: Design of steel structures, part 1–9: Fatigue (EN 1993-1-9)*. European Committee for Standardization.
- Fisher, J., & Barsom, J. (2016). Evaluation of cracking in the rib-to-deck welds of the Bronx-Whitestone bridge. *Journal of Bridge Engineering*, 21(3), 1–10. [https://doi.org/10.1061/\(ASCE\)BE.1943-5592.0000823](https://doi.org/10.1061/(ASCE)BE.1943-5592.0000823)
- Inokuchi, S., Ishii, H., & Ishigaki, T. (2010). Fatigue assessment for weld between deck plate and U-rib in orthotropic steel decks with consideration of pavement properties. *Doboku Gakkai Ronbunshuu A*, 66, 79–91.
- Ishii, H., Inokuchi, S., Kasugai, T., Murakoshi, J., & Yanadori, N. (2013). Study on fracture behavior of steel fiber reinforced concrete pavement for orthotropic steel deck. *Kozo Kagaku Ronbunshu A*, 59A, 1138–1149.
- Jiang, X., Su, Q., Han, X., Shao, C., & Liang, C. (2017). Experimental study and numerical analysis on mechanical behavior of T-shape stiffened orthotropic steel-concrete composite bridge decks. *International Journal of Steel Structures*, 17(3), 893–907. <https://doi.org/10.1007/s13296-017-1231-8>
- Ju, X., Zeng, Z., Zhao, X., & Liu, X. (2018). Fatigue study on additional cutout between U shaped rib and floorbeam in orthotropic bridge deck. *Steel and Composite Structures*, 28(3), 319–329. <https://doi.org/10.12989/scs.2018.28.3.319>
- Kainuma, S., Jeong, Y., & Ahn, J. (2015). Stress distribution on the real corrosion surface of the orthotropic steel bridge deck. *Steel and Composite Structures*, 18(6), 1479–1492. <https://doi.org/10.12989/scs.2015.18.6.1479>
- Ke, L., Li, C., He, J., Lu, Y., & Liu, Y. (2021). Fatigue evaluation and CFRP strengthening of diaphragm cutouts in orthotropic steel decks. *Steel and Composite Structures*, 39(4), 453–469. <https://doi.org/10.12989/scs.2021.39.4.453>
- Kodama, T., Kagata, M., & Higashi, I. (2010). Effect of reducing strains by SFRC pavement on orthotropic steel deck of Ohira viaduct. *Kozo Kagaku Ronbunshu A*, 56A, 1249–1258.
- Krstulovic, O., Haghayeghi, A., Haidar, M., & Krauss, P. (1995). Use of conventional and high-performance steel fiber reinforced concrete for bridge deck overlays. *American Concrete Institute*, 92(6), 669–677.
- Liu, Y., Zhang, Q., Bao, Y., & Bu, Y. (2020). Fatigue behavior of orthotropic composite deck integrating steel and engineered cementitious composite. *Engineering Structures*, 220, 111017. <https://doi.org/10.1016/j.engstruct.2020.111017>
- Lok, T., & Xiao, J. (1999). Flexural strength assessment of steel fiber reinforced concrete. *Journal of Materials in Civil Engineering*, 11(3), 188–196. [https://doi.org/10.1061/\(ASCE\)0899-1561\(1999\)11:3\(188\)](https://doi.org/10.1061/(ASCE)0899-1561(1999)11:3(188))
- Luiz, A., Oliveira, J., Vanessa, E., Alice, R., Daiane, V., Daniel, D., Mounir, K., & Paulo, F. (2010). Stress-strain curves for steel fiber-reinforced concrete in compression. *Materia*, 15(2), 260–266.
- Maljaars, J., Paulissen, J. (2016). Validation of a crack growth model using observed cracks in a bridge. In *119th IABSE Congress Stockholm*
- Miki, C., Suzuki, K., Kano, T., Sasaki, E., & Ishida, M. (2006). Preventive works for fatigue damage in orthotropic steel bridge deck by SFRC pavement and long term monitoring of the composite action. *Journal of Japan Society of Civil Engineers (A1)*, 62(4), 950–963.
- MTPRC. (2015). *Specification for design of highway steel bridge*. People Communications Press.

- Murakoshi, J., Kinomoto, T., Kasugai, T., & Kodama, T. (2013). Experimental study on performance evaluation of SFRC overlays as a measure to improve durability of existing orthotropic steel decks. *Journal of Japan Society of Civil Engineers (A1)*, 69(3), 416–428.
- Murakoshi, J., Kosuge, T., Ishii, H., Kasugai, T., & Toyama, N. (2012). Study on retrofit effect by SFRC overlay for existing orthotropic steel deck with fatigue crack through rib-to-deck weld. *Journal of Japan Society of Civil Engineers (A1)*, 68(3), 722–737.
- Noguchi, H., Abe, T., Kawai, Y., Yamashita, T., & Ichinose, Y. (2016). Decreasing effect of stress and evaluation of fatigue resistance in steel deck of SFRC pavement with rapid hardening cement or ordinary cement and low shrinkage type mixture material. *Journal of the Structural Engineering, American Society of Civil Engineers*, 62A, 1226–1239.
- Ono, S., Hirabayashi, Y., Shimozato, T., & Inaba, N. (2009). Fatigue properties and retrofitting of existing orthotropic steel bridge decks. *Journal of Japan Society of Civil Engineers (A1)*, 65(2), 335–347.
- Ono, S., Shimozato, T., & Masui, T. (2005). (2005), "Retrofitting method for existing orthotropic steel deck" *Doboku Gakkai Ronbunshuu*, 801, 213–226.
- Pei, B., Li, L., Shao, X., Wang, L., & Zeng, Y. (2018). Field measurement and practical design of a lightweight composite bridge deck. *Journal of Constructional Steel Research*, 147, 564–574. <https://doi.org/10.1016/j.jcsr.2018.05.005>
- Walter, R., Olesen, J., Stang, H., & Vejrum, T. (2007). Analysis of an orthotropic deck stiffened with a cement based overlay. *Journal of Bridge Engineering*, 12(3), 350–363. [https://doi.org/10.1061/\(ASCE\)1084-0702\(2007\)12:3\(350\)](https://doi.org/10.1061/(ASCE)1084-0702(2007)12:3(350))
- Yamada, K., Ya, S., Xiao, Z. (2005), Fatigue assessment of orthotropic steel deck case study: trough-to-deck detail. *8th Japan-Korea Seminar on Steel Bridges*. Japan
- Ye, H., Huang, R., Tang, S., Zhou, Y., & Liu, J. (2022). Determination of shear stiffness for headed-stud shear connectors using energy balance approach. *Steel & Composite Structures*, 42(4), 477–487.
- Ye, H., Wang, Y., Zhang, Q., Liu, Y., & Ai, Z. (2017). Full-scale fatigue test of new steel-concrete composite orthotropic bridge deck. *Journal of Harbin Institute of Technology*, 46(9), 25–32.
- Ye, H., Yang, Z., Han, B., Duan, Z., & Zhou, Y. (2021). Failure mechanisms governing fatigue strength of steel-SFRC composite bridge deck with U-Ribs. *Journal of Bridge Engineering*, 26(4), 1–9. [https://doi.org/10.1061/\(ASCE\)BE.1943-5592.0001692](https://doi.org/10.1061/(ASCE)BE.1943-5592.0001692)

Publisher's Note

Springer Nature remains neutral with regard to jurisdictional claims in published maps and institutional affiliations.

Submit your manuscript to a SpringerOpen[®] journal and benefit from:

- Convenient online submission
- Rigorous peer review
- Open access: articles freely available online
- High visibility within the field
- Retaining the copyright to your article

Submit your next manuscript at ► [springeropen.com](https://www.springeropen.com)
